TS-Fuzzy Controller based Grid Connected Hybrid Renewable Energy Sources

Siva Ganesh Malla*[1] and Priyanka Malla[2]
[1]Director, CPGC Pvt. Ltd., Visakhapatnam, Andhra Pradesh, India. Email: mallasivaganesh@gmail.com
[2]Jr. GIS Engineer, InfoTech, Cyient Ltd., Vizag, Andhra Pradesh, India, Email: priyamallaece@gmail.com

***Abstract*— Renewable energy based grid connected systems are popular nowadays. The combination of two or more renewable energy sources can provide reliable power to consumers as well as to grid. The photovoltaic (PV) and PMSG based wind power generation systems are famous worldwide. However, the wind power depends on velocity of wind and PV power depends on solar irradiance. Hence power generation from wind and PV will be always fluctuating due to atmospheric and weather changes. These changes are rapidly changed and unpredictable, an energy storage device is required in order to minimize the fluctuations in power generation from PV and wind. Battery is the best and effective energy storage device to reduce the fluctuations in the system with proper controller. Compare to Proportional and Integral (PI) and Mamdani Fuzzy controller, Takagi Sugeno-Fuzzy (TS-Fuzzy) controller can work effectively for rapid changes in system. The TS-Fuzzy based DC side and AC side controllers are proposed in this paper. The battery is connected to dc-link through bidirectional DC to DC converter and its controller is developed to regulate the dc-link voltage as well as to operate the Maximum power point tracker (MPPT) converter of PV system. The novel controller is developed for an inverter to connect the wind-PV-Battery based hybrid system to grid. The proposed controller can helps to compensate reactive power required by load, reduce the harmonics due to nonlinear load and maintain balanced grid currents during unbalanced load connected to PCC. The same inverter can also work to transfer active power to grid as well as act as MPPT of PV when State of Charge (SoC) of battery reaches its upper limit. Extensive results are presented with MATLAB to test the controllers under different case studies.**

Keywords— TS-Fuzzy, Renewable Energy Sources, PV, Wind, Grid, Battery, MPPT, DSTATCOM, Unbalanced Load

I. INTRODUCTION

The utilization of renewable energy sources are increasing day-by-day. Since the attention towards increasing pollution and problems of fossil fuels, the researchers are working towards designing of renewable energy based electrical power generation systems from last decades [1-4].

The renewable energy sources based grid connected power systems are very much famous and required more research for better performance. Among many renewable energy based systems, a wind and PV systems are attracting researchers towards new inventions due to its utilization and benefits [1-4]. The PV and wind turbine based power generation systems are mostly using in grid connected systems. However, both the sources are dependent on weather conditions and rapidly changes in nature [1-7]. Similarly the load is also rapidly changed due to need of customers. So, an energy storage device is required to compensate the power generation by these renewable energy sources to minimize the effect due to rapid changes. The high energy density rechargeable batteries are commonly using as energy storage devices in such a power generation systems to achieve better performance under various conditions. The main challenges in this type of renewable energy sources based grid connected system are to get reliable and maintain good power quality under all aspects and must be cost effective.

Due to their high efficiency and the ability to capture more power from the wind and PV by using maximum power point tracer (MPPT) converter with proper MPPT algorithms are used [1-7]. Generally, wind velocity and solar irradiance will not be constant always and depends on weather conditions. Hence, electrical power generation from wind and solar always fluctuates, so that storage devices are very essential and plays a vital role in stabilizing the power between the generating positions to load position especially under islanding mode in grid connected systems. Under this condition battery satisfies the load and under the condition of high power generated from Wind generator or (and) PV, then battery is charged along with satisfying the load. Generally, loads connected to point of common coupling (PCC) in distribution system are combination of unbalanced, linear, nonlinear and reactive power connected by both 1-phase and 3-phase. These types of loads are causes power quality issues as well as create problem to grid [8]. Hence, proper inverter controller is required to mitigate those problems in grid connected system.

Many researchers are proposed similar kind of systems, however, the proposed controller is unique in nature to solve many issues occurred in grid connected system. Generally, proportional and integral (PI) based controllers are unable to solve the issues presented due to rapid changes from source and loads in grid connected renewable energy based hybrid systems. The proposed DC side and inverter controller are designed by using TS-Fuzzy, it is having some significance over general or Mamdani Fuzzy [6, 9]. The detailed modeling, control strategies, system description and results

Article details: Received: August 25, 2019; Revised: March 19, 2020, Accepted: May, 23, 2020, Publication: July 10, 2020.

Citation of paper: Siva Ganesh Malla and Priyanka Malla, "TS-Fuzzy Controller based Grid Connected Hybrid Renewable Energy Sources", *International Journal of New Technologies in Science and Engineering (IJNTSE)*, Vol. 7, Issue. 7, pp. 1-13, July 2020.

*Corresponding author: Dr. Siva Ganesh Malla

under various conditions are discussed by following sections in this paper.

II. Description of the System

The grid connected hybrid PV-wind-battery based electrical power generation system is shown in Fig. 1. The permanent magnet synchronous generator (PMSG) is coupled with wind turbine by shaft for 3-phase electrical power generation. The PMSG based electrical power generation from variable speed wind energy conversion system is popular over doubly fed induction generator (DFIG) for small and medium power range. PMSG has received much attention and attracts researchers due to absence of gearbox, high power factor and efficiency. As PMSG produces AC output power, a diode rectifier is used to convert AC to DC. To extract the maximum power from wind turbine, a boost converter is used as MPPT converter in this system. The battery is connected to dc-link through bidirectional DC-DC converter. The PV system is directly connected to dc-link without using any extra MPPT converter. The controller of bidirectional DC-DC converter is designed such a fashion that it can work as MPPT converter for PV system. Hence there will not be use of any extra converter to extract maximum power from PV system. Perturbed and observe (P&O) algorithm is incorporated to bidirectional DC-DC converter of battery. Therefore, bidirectional DC-DC converter helps to regulate dc-link voltage corresponding to voltage at maximum power of PV system. Hence, no more extra converter is required to track maximum power point for PV system, it stated that the bidirectional DC-DC converter will also acts as MPPT converter for the PV system. Once regulating the dc-link voltage at its reference value, the inverter controller can helps to supply power to grid through inverter. The inverter is used to supply power from dc-link to grid. The output of inverter is connected to grid with the help of LC filter, PCC, transformer and π-transmission line. The different kinds of loads are connected to PCC as shown in Fig. 1. Most of the loads in distribution systems are 1-phase. The proposed inverter controller will operate the inverter to mitigate the problems occurred due to loads connected at PCC. For example, if the reactive power consumed by the load at PCC then proposed inverter controller can compensate the required reactive power by acting as DSTATCOM. The detailed use and aim of the proposed controllers are discussed briefly in next section. Before that, the detailed designing and modeling of components used in Fig. 1 is presenting below.

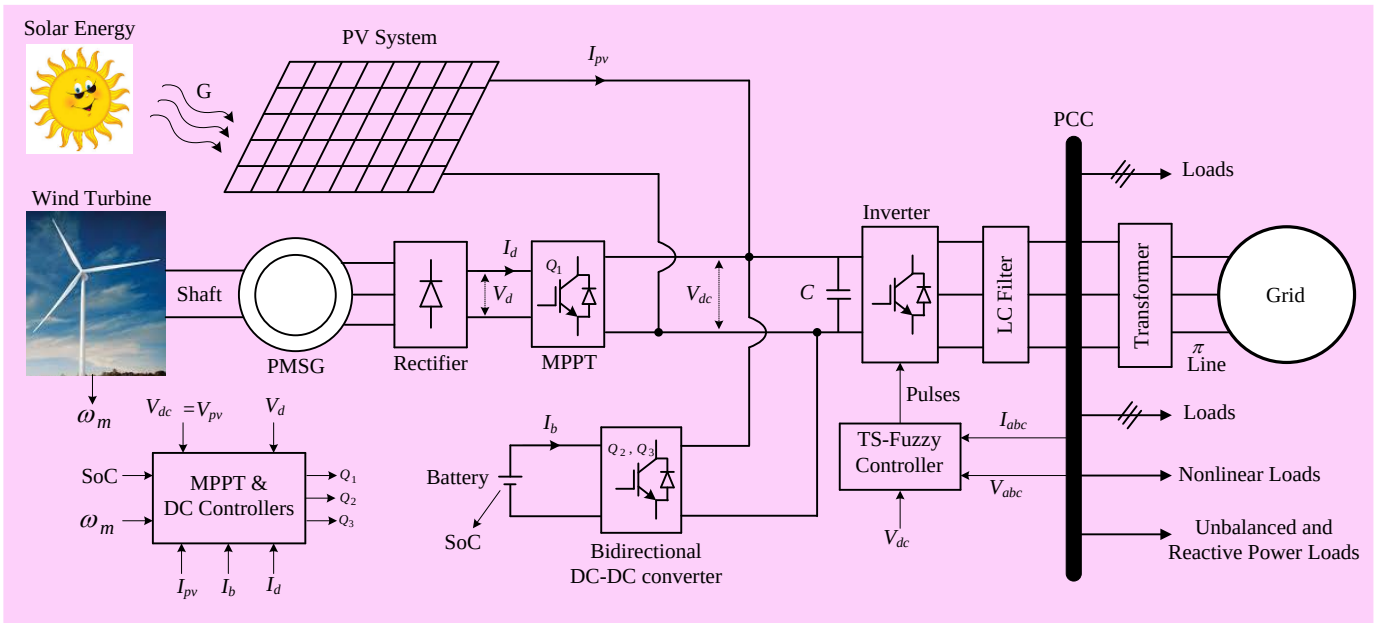

Fig. 1: Grid connected hybrid PV-Wind-Battery based electric power generation system

A. *Designing of LC Filter* [4, 10]

To produce proper output from PWM inverter, proper designed L-C filter is required. However, this filter works as a passive filter. The L-C filter design is based on following equations [4, 10]:

$$K = [(k^2 - \frac{15}{4}k^4 + \frac{64}{5\pi}k^5 - \frac{5}{4}k^6)/1440]^{1/2} \quad (1)$$

$$L_f = \frac{V_o}{I_o f_s}\left\{K\frac{V_{dc}}{V_{o,av}}\left[1+4\pi^2\left(\frac{f_r}{f_s}\right)^2 K\frac{V_{dc}}{V_{o,av}}\right]\right\}^{1/2} \quad (2)$$

$$C_f = K\frac{V_{dc}}{L_f f_s^2 V_{o,av}} \quad (3)$$

where, k (modulation index)=1;

V_o (Load voltage) = $400/\sqrt{3}$ V;
I_o (Nominal current) =30A;
f_r (Fundamental frequency) = 50 Hz;
f_s (Switching frequency) = 3 kHz;
$V_{o,av}$ (Total harmonic load voltage) = 5% of V_o ;
L_f = Inductance of filter; C_f = Capacitance of filter.

B. *Modeling of PMSG, Wind Turbine and Drive Train:*

The modeling of wind turbine and PMSG is achieved by [2-4, 11-13]. Wind speed (v) and pith angle (β) are considered to be inputs to the modeling of wind turbine. The attempt to modeling and design of wind turbine is done by below equations. The modeling is attempted to calculate mechanical torque generated by wind turbine is shown in Fig. 2. The

angular speed of the wind turbine (ω_t) is taken from two mass drive train model which is shown in Fig. 3. All the values are converted into nominal or per unit system while designing the wind turbine model. The function *f(x)* is evaluated from below equation.

$$f(x) = C_p = C_1\left(\frac{C_2}{\lambda_i} - C_3\beta - C_4\right)\exp\left(-\frac{C_5}{\lambda_i}\right) + C_6\lambda \qquad (4)$$

Where, $\lambda_i = \dfrac{1}{\dfrac{1}{\lambda + 0.08\beta} - \dfrac{0.035}{1+\beta^3}}$, C_1, C_2, C_3, C_4 and C_6 are constants.

The values in Fig. 2 can be calculated by below equations.

$$k_n = -\frac{\left(\frac{C_2C_5}{\lambda_{in}} - C_4C_5 - C_2\right)\exp\left(-\frac{C_5}{\lambda_{in}}\right)}{\lambda_n^2}$$

$$C_1 = \frac{C_{pn}}{\left(\frac{C_2}{\lambda_{in}} - C_4\right)\exp\left(-\frac{C_5}{\lambda_{in}}\right) + k_n\lambda_n}$$

$C_6 = C_1k_n$, where, $\lambda_{in} = \dfrac{1}{\dfrac{1}{\lambda_n} - 0.035}$

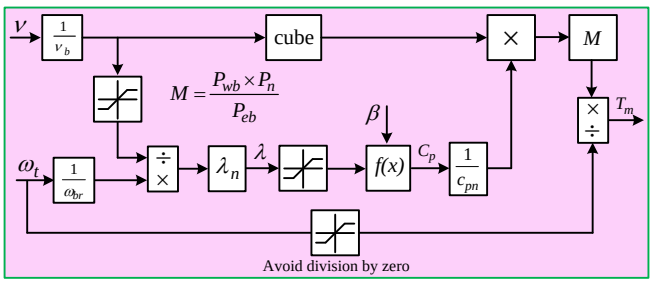

Fig. 2: Modeling of wind turbine

For more realistic performance of wind turbine, a two-mass drive train model shown in Fig. 3 is integrated to wind turbine model which is shown in Fig. 2. The modeling of two mass drive train can be achieved by following differential equations mentioned below.

$$2H_t\frac{d\omega_t}{dt} = T_m - T_{sh} \qquad (5)$$

$$\frac{1}{\omega_{elb}}\frac{d\theta_{tw}}{dt} = \omega_t - \omega_r \qquad (6)$$

where, H_t is the inertia constant of the turbine, θ_{tw} is the shaft twist angle, ω_t is the angular speed of the wind turbine in p.u., ω_r is the rotor speed of the PMSG in p.u., ω_{elb} is the electrical base speed, and the shaft torque T_{sh} is

$$T_{sh} = K_{sh}\,\theta_{tw} + D_t\frac{d\theta_{tw}}{dt} \qquad (7)$$

where, K_{sh} is the shaft stiffness and D_t is the damping coefficient.

The mechanical torque output obtained from Fig. 2 is taken as input to two mass drive train [4]. The detailed parameters and rating of wind turbine and two mass drive system are presented in Table-1.

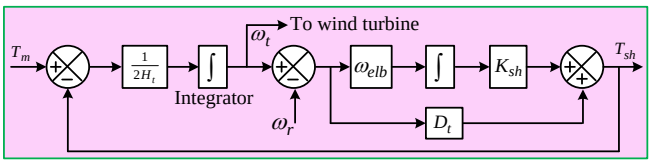

Fig. 3: Modeling of Two mass drive train

While modeling the above modules, considered all are in per unit system. Hence, the generated shaft torque T_{sh} should multiply by actual shaft torque generated by turbine. After multiplication by turbine torque, the output signal will be input torque signal of PMSG generator.

Therefore, $T_{sh-PMSG} = T_{sh} \times \dfrac{P_{wind}}{\omega_{base}}$

Here, $P_{wind} = P_{wb}$ is the equivalent electrical rated power generated by wind turbine. ω_{base} is the base speed of turbine shaft can be calculated from equations (8) to (12). The ω_{base} is slightly different from ω_{br} where ω_{br} is the base rotor speed or rated speed of PMSG.

In order to obtain maximum power from turbine it should operate at maximum value of C_p (i.e., at C_{p_opt} noted as C_{pm}). The turbine power vs wind turbine speed and C_p vs λ are depicted in Fig. 4. From the Fig. 4 (a) and (b), the wind turbine can generate maximum power by operating the turbine at particular speed, it can be obtained from C_{p_opt} and λ_{opt}. Therefore, it is necessary to keep the rotor speed at an optimum value of the tip-speed ratio λ_{opt}. If the wind speed varies, the rotor speed should be adjusted to follow the change.

The wind turbine needs a device to track the maximum power. However, the turbine is directly connected to PMSG without any gear system, the wind turbine speed can be controlled by controlling speed of PMSG with the help of load current. This can be helps to design an electrical device such as boost converter to control the speed of PMSG by regulating load current or DC current after rectifier as shown in Fig. 1. The MPPT logic and controller is designed by following equations:

$$P_t = 0.5\rho AC_p(\lambda,\beta)v^3 \qquad (8)$$

Where, ρ is air density, v is wind speed, A is blade's swept area and C_p is turbine-rotor power coefficient.

$$T_m = \frac{P_t}{\omega_t} \text{ And } \lambda = \frac{\omega_t}{v} \qquad (9)$$

Where λ is tip speed to wind speed ratio.

For maximum power tracking, $\lambda = \lambda_{opt} = \lambda_m = \text{constant}$

$$\frac{\omega_{t1}}{v_1} = \frac{\omega_{t2}}{v_2} \qquad (10)$$

Moreover, if wind energy conversion system is under MPPT in steady state,

$C_p = \text{contant} = 1\,\text{p.u.}, \text{and}$ ρ, A are constant

$\therefore T_m\,\alpha = \dfrac{v^3}{\omega_t}$ Therefore, finally, $\dfrac{T_{m1}}{T_{m2}} = \dfrac{v_1^2}{v_2^2}$

The optimal or maximum power can be calculated by below equations:

$$P_{tm} = 0.5\rho AC_{pm}\left(\frac{\omega_{tm}R}{\lambda_m}\right)^3 = K_m(\omega_{tm})^3 \qquad (11)$$

Where, $K_m = 0.5\rho AC_{pm}\left(\frac{R}{\lambda_m}\right)^3$; $\omega_{tm} = \frac{\lambda_m}{R}v$; R is radius of the turbine.

Therefore, the target optimal torque can be calculated by

$$T_{tm} = K_m\omega_{tm}^2 \qquad (12)$$

Here, T_{tm} is the reference torque of wind turbine calculated for maximum power.

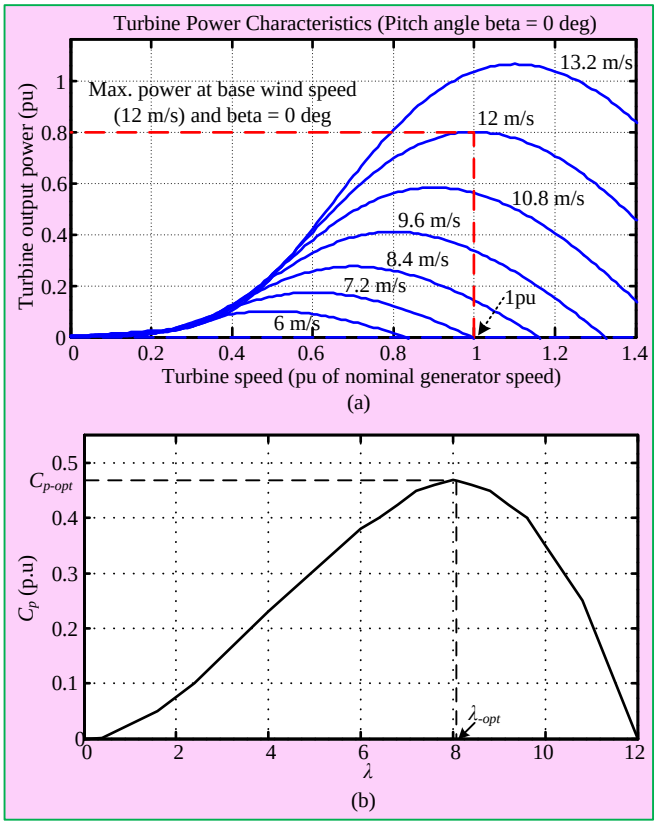

Fig. 4: (a) power vs speed; (b) turbine-rotor power coefficient vs tip speed to wind speed ratio

However, the MPPT of wind is designed from PMSG, since wind turbine speed can be controlled by PMSG rotor. Hence the reference shaft torque of PMSG should be followed by

$$T^* = K_m\omega_{tm}^2 - j\frac{d\omega_{tm}}{dt} - D\omega_{tm}$$

Hence, the power generated by PMSG is

$$P_{PMSG} = \omega_r \times T^*$$

Where, ω_{tm} turbine speed at maximum power, J and D are the inertia and damping constants of PMSG.

The generated power from PMSG should be transferred to DC side through rectifier. However, considered lossless and unity conversion system of rectifier, the DC side power should be same as power generated by PMSG. By measuring DC voltage at rectifier, easily can calculate reference current from P_{PMSG} and V_d by

$$I_d^* = \frac{P_{PMSG}}{V_d} = \frac{\omega_m \times T^*}{V_d}$$

While measuring V_d, an effective capacitor with proper value needs to be connected across rectifier. To avoid the pulsations in current and voltage of rectifier, proper filter also required after measuring voltage and current.

The model of MPPT algorithm or technique along with its controller for boost converter is shown in Fig. 5.

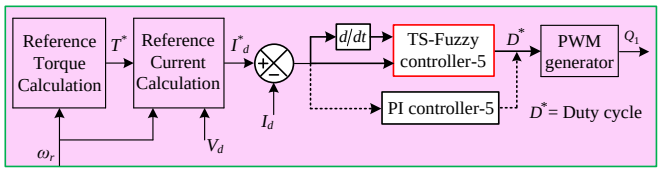

Fig. 5: MPPT technique with controller for boost converter

The PMSG rotor speed is used to calculate the reference torque and reference current will follow by reference torque. The generated reference current is comparing with actual value of current. The error is giving to TS-Fuzzy controller/PI controller to generate the required duty cycle. The gate pulses for switch Q_1 is generating from duty cycle with the help of PWM generator as shown in Fig. 4. However, for rapid changes in wind velocity and changes in current flow thorough rectifier due to changes in load, the PI cannot perform well compare to TS-Fuzzy. Hence, the TS-Fuzzy based controller can provide smooth operation while tracking the maximum power from wind under changes in weather and load. Furthermore, it can help to reduce the ripples in DC of boost converter to protect the dc-link bus. The reduction in ripples can allow more sources for interconnecting to dc-link bus, such as PV, battery and other renewable sources or loads [14-15]. Furthermore, this TS-Fuzzy controller can able to supply quality power to DC loads which are connected to dc-link by minimizing the ripples (smooth voltage and current) [6, 9]. Moreover, by minimizing the oscillations in dc-current, it will reduce the oscillations in rotor of the PMSG. The PMSG rotor is directly coupled with wind turbine so that the oscillations in wind turbine can minimize with proposed TS-Fuzzy based controller. The reduction in oscillations in shaft can improve the life of both PMSG and wind turbine.

Modeling and designing of PMSG is carried out from [2-4, 11-13]. The modeling of PMSG can easily achieve by d-q reference theory. The parameters of PMSG are provided in Table-2.

Table 1: Parameters of wind turbine and two mass drive train

H_t	4s
H_g	0.1Ht
K_{sh}	0.3 p.u./el.rad
D_t	0.7 p.u.s/el.rad
Density of air	1.255 Kg/m^3
Area swept by blades	1.06 m^2
Optimum coefficient K_{opt}	1.678x10^{-3} Nm/(rad/s)^2
Base wind speed	12 m/s

Table 2: Parameters of PMSG

Number of poles	10
Rated speed	153 rad/s
Armature resistance (Rs)	0.425 Ω
Magnetic flux linkage	0.433 Wb
Stator inductance (Ls)	8.4 mH
Rated current	12 A
Rated torque	40 Nm
Rated power	6 kW

C. PV System [5, 7, 9, 16-18]

PV cell is a device that can directly converts the energy of solar or light into electricity by the photovoltaic effect. A PV cell is described by current-voltage characteristic function as:

$$I_{pv} = I_{ph} - I_{rs}\left[\exp\left(\frac{q\left(V_{pv} + I_{pv}R_s\right)}{AKT}\right) - 1\right] - \frac{\left(V_{pv} + I_{pv}R_s\right)}{R_{sh}} \quad (13)$$

where,

$$I_{rs} = I_{rr}\left[\frac{T}{T_r}\right]^3 \exp\left(\frac{qV_D}{AK}\left[\frac{1}{T_r} - \frac{1}{T}\right]\right), \; I_{ph} = \left[I_{sc} + k\left(T - T_r\right)\right]\frac{G}{1000}$$

where q=1.602·10^{-19} C is the electron charge, K=1.3806·10^{-23} J/K is Boltzmann's constant, A=2 is the p-n junction's idealistic factor, T is the cell's temperature (K), T_r is the reference room temperature (K), I_{ph} is the cell's photocurrent (it depends on the solar irradiation and temperature), I_{rs} is the cell's reverse saturation current, G is the solar irradiance and V_{pv} is cell voltage V_D is the voltage across the diode, R_s is cell internal series resistance, R_{sh} is cell shunt resistance, k is the short circuit current-temperature factor, and I_{pv} is cell current.

The schematic diagram of a PV cell is shown in Fig. 6(a). However, a single solar cell cannot produce sufficient voltage and current. In order to increase the voltage and current, many solar cell where connected in combination of series and parallel to form a PV module. The PV array is shown in Fig. 6(b), here, I_{PV} and V_{PV} are the PV array's current and voltage respectively. Based on current-voltage requirement, the PV array can design and manufacture. According to our power rating, the number of PV module/arrays will be selected. The detailed modeling of PV array can be divided into voltage based and current based models. PV array's current (IPV) is the input parameter of eq. (11) while doing modeling. In similar way, the voltage of PV array will be the input parameter for current based PV array modeling. Since, only one PV current-voltage characteristic equation is available with two parameters are variables such as current and voltage. Therefore, one parameter should be taken as input to the model while designing the modeling of PV array. The voltage based modeling of PV array is shown in Fig. 7. The system is modeling for one cell by using eq. (11) and converted to PV array model by using number of cells connected in parallel (n_p) and number of modules connected in series (n_s). The n_p can increase the rating of current and n_s is for increasing the voltage as per as our requirement. The listed parameters of PV systems are depicted in Table-3.

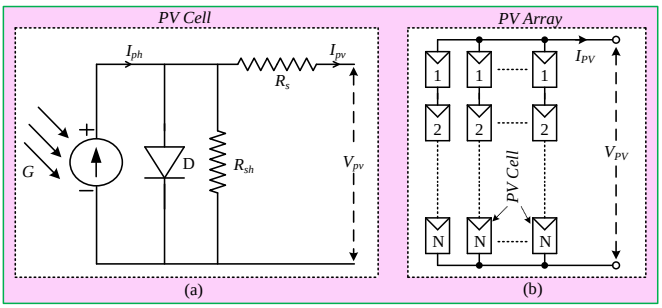

Fig. 6: Schematic Diagram of (a) PV Cell and (b) PV array

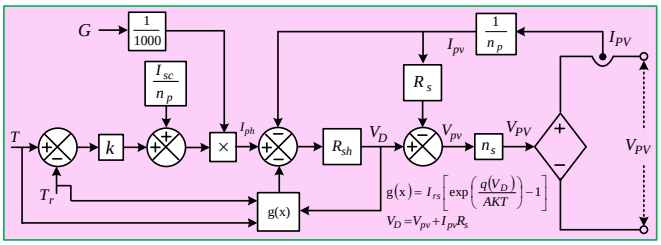

Fig. 7: Detailed modeling of PV array

Table 3: Parameters of PV

Open circuit voltage of module V_{oc}	36.90 V
Short circuit current of module I_{sc}	8.01 A
Voltage at maximum power V_{mpp}	30.3 V
Current at maximum power I_{mpp}	7.10 A
Series resistance R_s	0.0045
Shunt resistance R_{sh}	0.9822
Cell diode voltage V_D at MPP V_{dm}	0.5367
No. of cells connected in parallel/module	Vary*
No. of cells connected in series/module N_s	Vary**
Reference room temperature T_r	25^{0}C
Cell thermal voltage V_t	26mV
PN-junction diode current at MPP	0.3636
Reverse saturation current I_{rr} at T=T_r	3.94x10-^{10}
PN-junction diode voltage at MPP V_{dm}	0.5367
Number of modules connected in series n_s	22
Rated irradiance G*	1000 W/m^2
Rated power of PV array	4.73 kW

Note: Calculations of PV parameters:

Ns=Round (V_{oc}/0.61)

$$I_{dm} = I_{sc} - I_{mpp} - \frac{V_{dm}}{R_p}$$

$$I_{rr} = \frac{\left(I_{sc} - \frac{V_{oc}}{N_s R_{sh}}\right) \Big/ \left(\exp\left(\frac{V_{oc}}{N_s V_t}\right) - 1\right)}{\left[\frac{T}{T_r}\right]^3 \exp\left(\frac{qV_D}{AK}\left[\frac{1}{T_r} - \frac{1}{T}\right]\right)}$$

$$V_{dm} = V_t \times \log\left(I_{dm} / I_{rr} + 1\right)$$

$$R_s = \frac{\left(V_{dm} - \frac{V_{mpp}}{N_s}\right)}{I_{mpp}}, \; R_{sh} = \frac{\left(\frac{V_{mpp}}{N_s I_{mpp}} - R_s\right) \times R_p}{\left(R_p - \frac{V_{mpp}}{N_s I_{mpp}} + R_s\right)}$$

$$I_{pt} = \frac{V_t}{R_{sh}},\ R_p = \frac{V_{dm}}{\left(I_{sc} - I_{mpp} - I_{pt}\right)}$$

While calculating above parameters, the initial values needs to be fixed first and the process should repeat at least 10 iterations to get accurate values. The initial parameters are

$$R_p = 100 \times \frac{V_{oc}}{N_s I_{sc}} \text{ and } V_{dm} = \frac{V_{oc}}{N_s}$$

According to Power vs Voltage characteristics of PV system, PV can generate maximum power at particular operating voltage which is called as voltage at maximum power point (V_{mpp}) for particular irradiance. The Power vs voltage characteristics of PV array with different levels of irradiance are shown in Fig. 8 under consideration of uniform irradiance. Of the several algorithms proposed in the literature, the most popular technique is the perturbed and observe (P&O) algorithm and used extensively for the MPPT [5, 116-18]. This can be achieved by power electronics devices which can bale to regulate the dc voltage at V_{mpp} by proper controller.

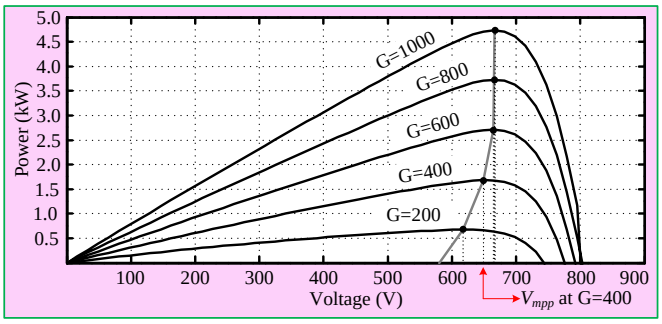

Fig. 8: Power-Voltage characteristics of PV system under various irradiances

In this implementation, the reference voltage (V_{mpp}) is generated by P&O method. Depending upon the sign of the change in power with respect to change in voltage, the direction for further perturbation is decided. A feedback control loop in converter controller ensures that the output voltage tracks its reference. The following equation is followed to locate the voltage at which the maximum power point (MPP) is reached.

$$V_{mpp}(k) = V_{mpp}(k-1) + \Delta V \times \text{sign}\left(\frac{dP_{PV}}{dV_{PV}}\right) \qquad (14)$$

where, ΔV is steep voltage and k is the iteration.

In order to regulate dc-link voltage, a bidirectional DC-dc converter is required [16-20]. Once V_{mpp} generated from P&O, this signal will become the reference dc-link voltage of DC-DC bidirectional converter controller. The detailed bidirectional DC-DC converter controller with integration of P&O algorithm is shown in Fig. 9. The limiter is used to limit the upper and lower value of V_{mpp}. This limiter cannot allow the reference signal to over voltage of dc-link voltage by limiting upper value. Hence, it will not be permit the dc-link voltage to protect the dc-link as well as DC loads connected to dc-link. Similarly, the limiter can also limit the reference dc-link voltage such as V_{mpp} to not reduce beyond the permissible lower limit. The lower limit can helps the inverter from over modulation as well as protection against weak dc-link. This lower limit value is useful to maintain the dc-link voltage at its lower limit value during night time, since there will not be any irradiance to generate the proper V_{mpp}. Therefore, the controller can work properly during all the conditions such as available and non available of irradiance. The lower and upper values of limiter can be set as per as our requirement by considering both the protection of dc-link as well as inverter from it's over modulation issues.

The error signal is generating by comparing actual dc-link voltage (V_{dc}) to V_{mpp}. This error signal is giving to TS-Fuzzy/PI controller to generate the reference battery current (I_b^*). The power mismatch between generation and load will reflect on dc-link voltage, therefore the reference battery current is generating from dc-link voltage and its reference value. The mismatch between load and generation power should be compensated by battery by either charging or discharging through bidirectional DC-DC converter. However, the grid will take the surplus power by limiting the charging power by battery. This can be achieved by using limiter after generating battery reference current from TS-Fuzzy/PI controller. By limiting the current, controller can also protects the battery from over charging and discharging current. This will improve the life time of battery. The battery reference battery current is comparing with actual battery current to generate the required pulses for switches Q_2 and Q_3 through hysteresis current loop. Moreover, the state of charge (SoC) of battery is also incorporated to pulses to stop the battery when SoC reaches its upper and lower limit. The complete controller for regulating d-link voltage through bidirectional DC-DC converter is shown in Fig. 9. From figure, it can say that the controller can also protects the dc-link, battery from over charging and discharging, inverter from over modulation as well as can able to supply smooth dc-link voltage to DC loads which are connected to dc-link. By integrating P&O algorithm with controller of DC-DC converter, the bidirectional convert can also acts as MPPT converter for PV. Hence, no more extra converter is required to extract maximum power from PV, it is a cost effective.

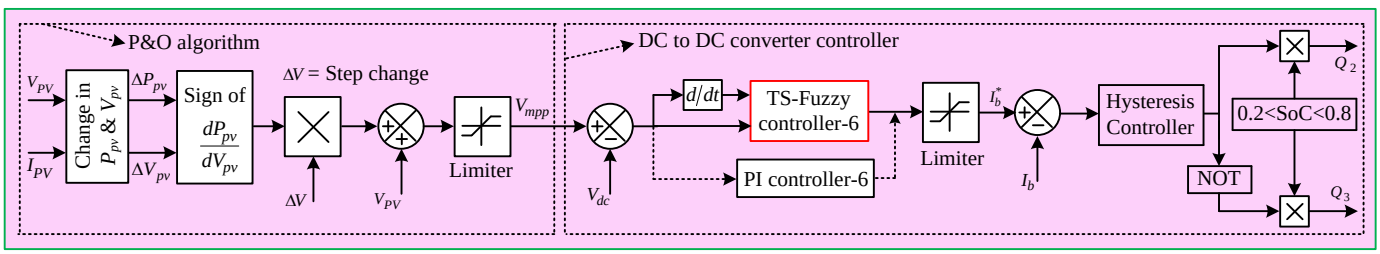

Fig. 9: Implementation of controller for bidirectional DC-DC converter associated with P&O algorithm

D. Modelling of a Battery

A temperature based generic battery model is implemented from [4-6, 16-18] in this paper. The temperature and SoC of battery are considered while modeling the battery. The modeling is attempted using a simple controlled voltage source with battery internal resistance (R_b) as shown in Fig. 10, where the controlled voltage source is described through below equations.

$$E_m = E_{m0} - K_E(273+\theta)(1-SOC) \quad (15)$$

$$Q_e(t) = Q_{e\_init} + \int_0^t -I_m(\tau)d\tau \quad (16)$$

$$I_p = V_{PN}G_{P0}\exp\left(\frac{V_{PN}}{V_{P0}(\tau_p s+1)} + A_P\left(1-\frac{\theta}{\theta_f}\right)\right) \quad (17)$$

$$C(I,\theta) = \frac{K_c C_{0*} K_t}{1+(K_c-1)(I/I^*)^{\delta}},\ K_t = LUT(\theta) \quad (18)$$

Where, $SOC = 1-\frac{Q_e}{C(0,\theta)}$, $DOC = 1-\frac{Q_e}{C(I_{avg},\theta)}$

$$\theta(t) = \theta_{init} + \int_0^t \frac{\left(Ps - \frac{(\theta-\theta_a)}{R_\theta}\right)}{C_\theta}d\tau$$

where, E_m and E_{mo} are the open-circuit voltage (V) and open circuit voltage at full charge (V) respectively, θ is electrolyte temperature (^{0}C), Q_e is the extracted charge (A S), Q_{e_init} is the initial extracted charge (A S), I_m is the main branch current (A), τ is an integration time variable, I_P is the current loss in parasitic branch, V_{PN} is the voltage at the parasitic branch, τ_P is a parasitic branch time constant, θ_f is electrolyte freezing temperature (^{0}C), C_{0*} is the no-load capacity at 0^0C, K_t is a temperature dependent look-up table, I^* is a nominal battery current, DOC is a depth of charge, C is the battery capacity (A-H), K_E, G_{P0} and δ are constants.

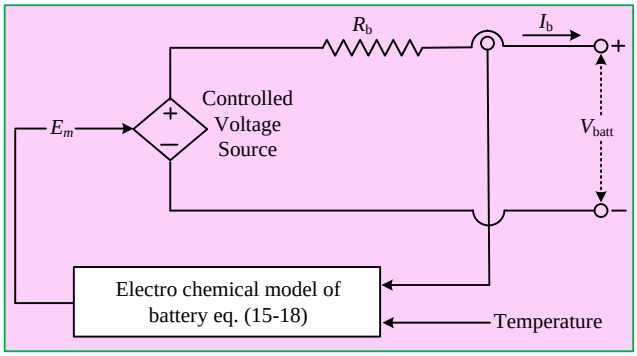

Fig. 10: Generic model of battery

The battery parameters are mentioned in Table-4. The rating of battery is selected by considering power rating of system as well as our requirement. The effective rating is considered by below equation:

$$\text{Capacity of battery } (I_{b\text{-}Ah}) = \frac{Power \times Time}{V_{bat} \times SoC_{avg}}$$

The following assumptions are attempted while calculating the rating. The battery needs to supply the power to load during islanding condition when there will not be any power available from PV and wind. This is the worst scenario of battery that needs to supply 10kW power continuously to the load connected at PCC for 24 hrs at the selected battery bank voltage of 300 with considered average SoC at 60%.

$$I_{b\text{-}Ah} = \frac{10000 \times 24 \times 100}{300 \times 60} = 1333\ Ah$$

Table-4: Parameters of battery

S.No	Parameter	Value
1	Nominal voltage	300
2	Rated capacity	1333
3	Average and initial SoC	60
4	Maximum capacity	1388.6
5	Fully charged voltage	327
6	Nominal discharge current	266.6
7	Internal resistance	0.0023
8	Battery response time	30
9	Battery type	Lead-acid

E. Implementation of TS-Fuzzy [6, 9]

The deviations in voltage/current error (x_i) and its derivative ($\dot{x}_i$) signal are taken as the input variables to designing the TS-Fuzzy control which is shown in Fig. 11. The error and its derivative input signals to TS-Fuzzy block are fuzzified by means of two linguistic memberships (MFs) values positive (P) and negative (N). The MFs of the two input linguist variables such as P and N for x_i and $\dot{x}_i$ signals are expressed by below functions:

$$\mu_P(x_i) = \begin{cases} 0, & x_i < L_1 \\ \frac{x_i + L_1}{2L_1}, & -L_1 \le x_i \le L_1 \\ 1, & x_i > L_1 \end{cases} \text{ and } \mu_N(x_i) = \begin{cases} 1, & x_i < L_1 \\ \frac{-x_i + L_1}{2L_1}, & -L_1 \le x_i \le L_1 \\ 0, & x_i > L_1 \end{cases}$$

$$\mu_P(\dot{x}_i) = \begin{cases} 0, & \dot{x}_i < L_2 \\ \frac{\dot{x}_i + L_2}{2L_2}, & -L_2 \le \dot{x}_i \le L_2 \\ 1, & \dot{x}_i > L_2 \end{cases} \text{ and } \mu_N(\dot{x}_i) = \begin{cases} 1, & \dot{x}_i < L_2 \\ \frac{-\dot{x}_i + L_2}{2L_2}, & -L_2 \le \dot{x}_i \le L_2 \\ 0, & \dot{x}_i > L_2 \end{cases}$$

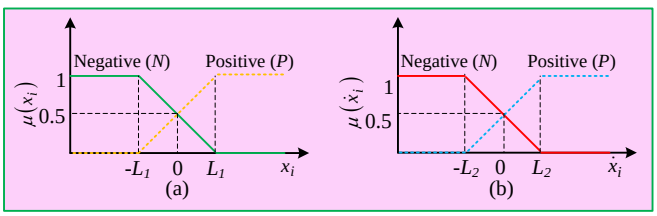

Fig. 11: Ts-Fuzzy membership functions

The corresponding rules for Ts-Fuzzy controller are provided in Table-5. The parameters used in Ts-Fuzzy are needs to be tuned and selected based on where the TS-Fuzzy used.

Table-5: The TS-fuzzy controller rules:

Rule	x_i(k)	$\dot{x}_i$(k)	Value
Rule-1	*N*	*N*	$Z_1 = a_1 x_i(k) + a_2 \dot{x}_i(k)$
Rule-2	*N*	*P*	$Z_2 = a_3 Z_1$
Rule-3	*P*	*N*	$Z_3 = a_4 Z_1$
Rule-4	*P*	*P*	$Z_4 = a_5 Z_1$

In the above rules, Z_1, Z_2, Z_3, and Z_4 represent the consequent of the TS-Fuzzy controller, k is the k^{th} sampling instant. a_1, a_2, a_3, a_4 and a_5 are the fuzzy constants. The values of the fuzzy constants are adjusted by tuning process and it's varying for one controller to another TS-Fuzzy controller.

The output of the TS-Fuzzy controller (Y) is obtained by using the generalized defuzzifier, which is evaluated by eq. (17).

$$Y = \frac{Z_1F_1 + Z_2F_2 + Z_3F_3 + Z_4F_4}{Z_1 + Z_2 + Z_3 + Z_4} \quad (19)$$

where, F_1= min. $\{\mu_p(x_i), \mu_p(\dot{x}_i)\}$, F_2= min.$\{\mu_p(x_i), \mu_N(\dot{x}_i)\}$, F_3= min. $\{\mu_N(x_i), \mu_p(\dot{x}_i)\}$, F_4= min. $\{\mu_N(x_i), \mu_N(\dot{x}_i)\}$

As the value of "*Y*" is adapted dynamically using the fuzzy based controller which results in improves the stability of power system with system events.

III. Control of Inverter

Inverter is required to synchronous the dc power to grid. The inverter controller can do the synchronization of output of inverter to grid with help of proposed controller. The priority taken as battery can charge from renewable energy sources and the amount of charging current can be limited through limiter which is used in Fig.9. If the availability of current is more from renewable energy side, then the DC current can flow through inverter by converting to AC. The load will be supplied from renewable energy source and surplus power will be compensated by grid. Once battery is fully charged or more generation available from DC side, then bidirectional DC-DC converter cannot regulate the dc-link voltage. Therefore, controlling of dc-link voltage is also incorporated with proposed inverter controller. Battery can effectively work under islanding condition and the limiter of DC-DC converter controller will be adjusted accordingly. Because, during islanding condition the battery needs to be compensate the surplus power between load and generation without limiting the current. During normal operation the power from wind and PV also considered to generate the reference active current component (i_d^*). This will helps to transfer active power from DC side to AC/grid side through inverter. The detailed proposed inverter controller is shown in Fig. 12. The reference reactive component of current (i_q^*) is generated from RMS voltages at PCC. This will help to compensate the reactive power consumed as well as regulating RMS voltage at PCC. The TS-Fuzzy is used to obtain the reference values of currents so that the smooth operation of system can be obtained during all possible changes in both DC side and AC side. The currents flowing through load will be depends on what type of load connected at PCC. Mostly, the distribution system consist combination of unbalance, reactive and nonlinear loads. Hence, the D-Q components of current are having some amount of harmonics and oscillations. While generating dc-component of D-Q currents, a low pass filter used. The reference current components i_d^* and i_q^* will be compare to actual current components i_d and i_q of PCC to generate reference voltage components through TS-Fuzzy respectively as sown in Fig. 12. Hence, the inverter can able to regulate both AC side as well as DC side and also able to compensate reactive power consumed at PCC. Therefore, the DSTATCOM operation of inverter controller can be achieved through inverter and its controller which is connected between dc-link and grid. This will help to not use of any extra inverter for DSTATCOM operation required by near substation of PCC. Hence, the controller can help to make system cost effective. In order to allow harmonics and oscillations from grid through inverter, the voltage components (v_d and v_q) and decoupling components ($\omega L i_{dh}$ and $\omega L i_{qh}$) are included while generating reference voltage components. By considering these harmonic component directly to generate the reference signals for generating pulses will helps the inverter to compensate or allowing the harmonic currents through inverter only. Hence, the harmonics and oscillations will be circulating through inverter only to minimize the effect of harmonics from grid currents. Therefore, the harmonic content from the nonlinear load which is connected to PCC is compensating by inverter and the inverter makes the harmonics free currents which are flowing through grid. This operation is similar to active power filter. Moreover, the proposed inverter controller can make balanced currents of grid under unbalanced load connected at PCC. Making balanced grid currents can helps to supply balanced voltage to other load points connected to grid. The voltage drop of three phase grid system will be equal by making the balanced currents flow through grid by inverter control, hence the receiving end voltage at grid becomes balanced. However, due to many changes occurring at PCC, the PI controllers cannot perform well due to their gains are tuned at particular instant. Due to ability of auto adjustments of gains by using TS-Fuzzy based controllers, the proposed controller can perform well to achieve all the objectives which are designed for controller of inverter. The reference voltage dc-components (v_d^* and v_q^*) are converted to reference 3-phase voltages (v_{abc}^*). These reference voltage signals are given to space vector pulse width modulation (SVPWM) technique for generating required pulses to inverter. SVPWM technique has advantage of an optimal output and also decreases harmonic content of inverter output.

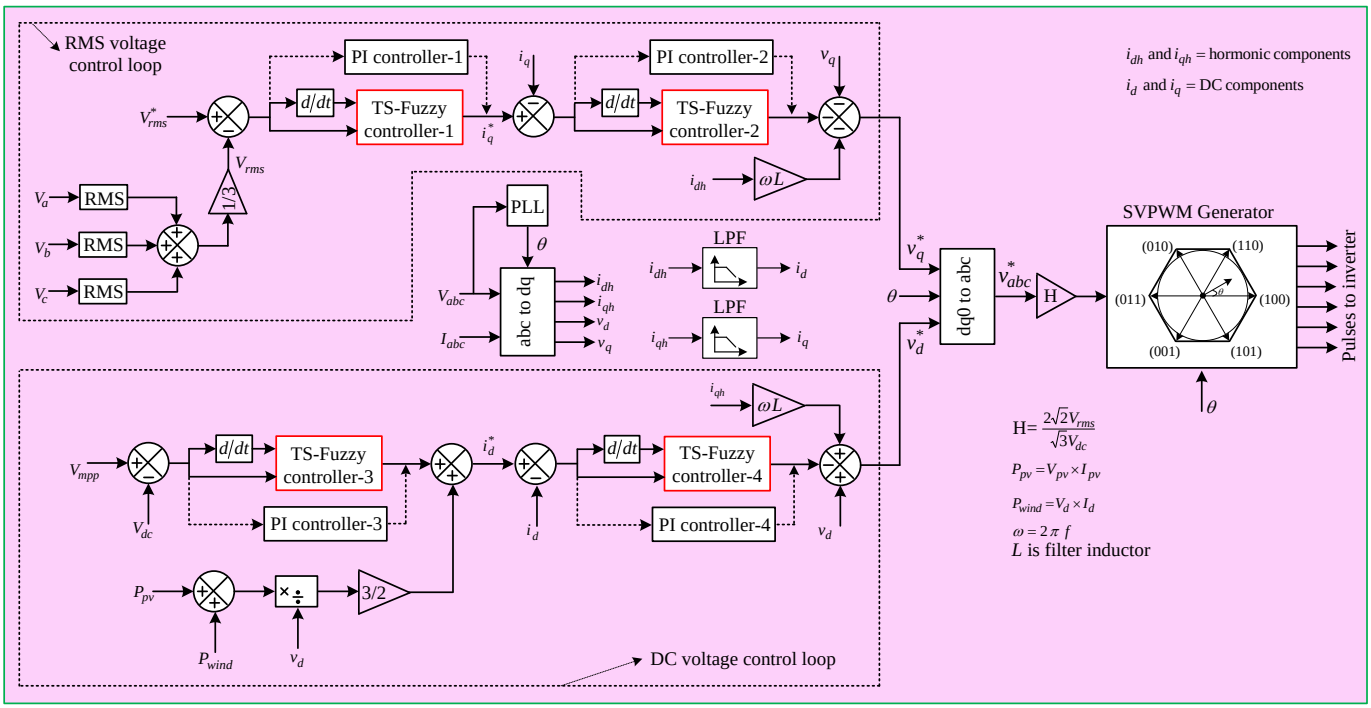

Fig. 12: TS-Fuzzy controller based proposed inverter controller for grid connected hybrid renewable energy sources

IV. Results and Discussions

The system results are carried out by Matlab 2013 version. The results with possible cases are discussed below.

Case-1: MPPT of wind and PV system:

The wind turbine and PV system requires MPPT to extract the maximum possible power from particular wind speed and solar irradiance respectively. Fortunately, wind turbine is directly coupled with PMSG shaft, hence the PMSG speed and wind turbine speed will be same. Hence, by regulating speed of PMSG will reflects the speed of wind turbine. Therefore, the MPPT controller is designed for PMSG to regulate the speed of wind turbine to extract the maximum power. From Fig. 4 and Fig. 5, the MPPT controller is implemented for boost converter to regulate the current corresponding to reference current which is generated by MPPT algorithm. As PMSG generates electrical power, the speed of generator shaft can be regulated by varying the electrical load on shaft, which is the same current flowing through rectifier. Hence, the boost convert can achieve the regulation of DC current by varying the duty cycle. Similarly MPPT of PV system also designed accordingly Fig. 8 and Fig. 9. In this case, considered solar irradiance is changed from 1000 w/m2 to 750 w/m^2. The performance is observed with using PI and TS-Fuzzy controller in Fig. 9. As bidirectional DC-DC converter is acting as MPPT controller and converter hence the MPPT tracking performance is depends on PI and TS-Fuzzy controller. As the gains of PI controller tuned at irradiance 1000 w/m^2, the PI controller can perform well at the point, but the same gains cannot work properly at irradiance 700 w/m^2. However, with TS-Fuzzy have the ability to adjust the output according to maximum power point. The reference power, actual power generated by PV with PI and TS-Fuzzy controller is depicted in Fig. 13. By observing Fig. 13, the performance of MPPT is well with TS-Fuzzy controller compare to PI controller for extracting maximum power from PV. The DC-DC converter is working for MPPT of PV system by regulating dc-link voltage (Fig. 9) at its reference value. Moreover, due to gains of PI which are not tuned at irradiance 700 w/m2 the oscillations are more in dc-link voltage. It will effect on tracking the maximum power from PV.

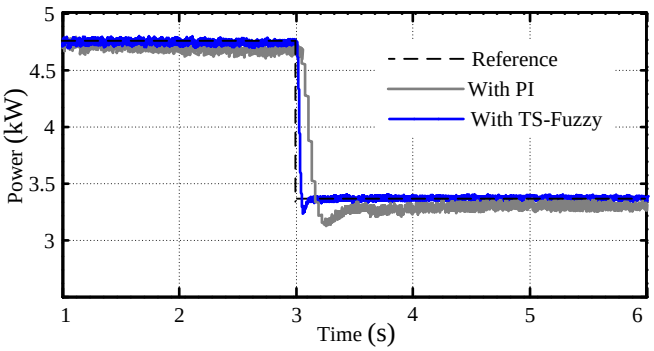

Fig. 13: MPPT performance of PV with PI and TS-Fuzzy

Similarly the MPPT of wind generator with PI controller and TS-Fuzzy controller is depicted in Fig. 14. While tracking the reference current of PMSG, TS-Fuzzy can perform well duet to adjustment of gains. Furthermore more power can be extracted from wind turbine with TS-Fuzzy controller. The power of PMSG depends on dc current of rectifier hence the tracking of the reference current from MPPT algorithm of wind generator reflected on power generation from wind turbine. The performance of MPPT is tested under changing of wind speed from 12 to 7 m/s. Hence concluded that the TS-Fuzzy based controller can provide better solution to this system. Hear after, the results are taken with only TS-Fuzzy.

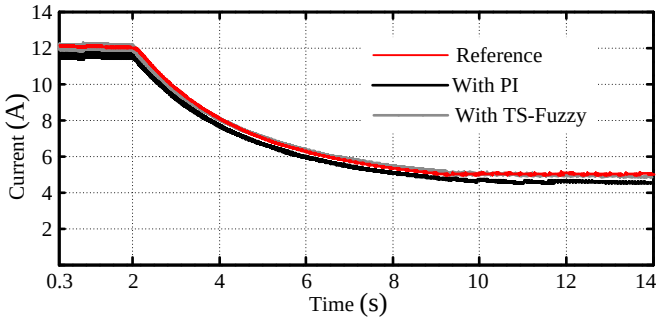

Fig. 14: Performance of wind turbine MPPT with PI and TS-Fuzzy

Case-2: changes in sources and load:

Considered changes in solar irradiance, wind speed and load consumption at PCC. For better realistic performance, considered 15 hours time period will all possible time conditions. The time period considered form starting at 7 AM to ending at night 10 PM. Generally the solar irradiance is low at early morning and evening timings. The irradiance is negligible during night time and maximum at during mid day. The profile of changing in solar irradiance and wind speed is followed in Fig. 15. According to Fig. 15, the time scaling factor used by considering 0 sec is the time at morning 7 o'clock, 15 sec is at 10 PM. Hence, the solar irradiance will reach at its maximum value (i.e. 1000 w/m^2) during time 5 sec to 7 sec (i.e., 12 AM to 2 PM). Similarly the irradiance is reaches its nominal value after 11 sec which is equals to 6 PM. The correspond powers of load, PV, wind, battery and grid has depicted in Fig. 16.

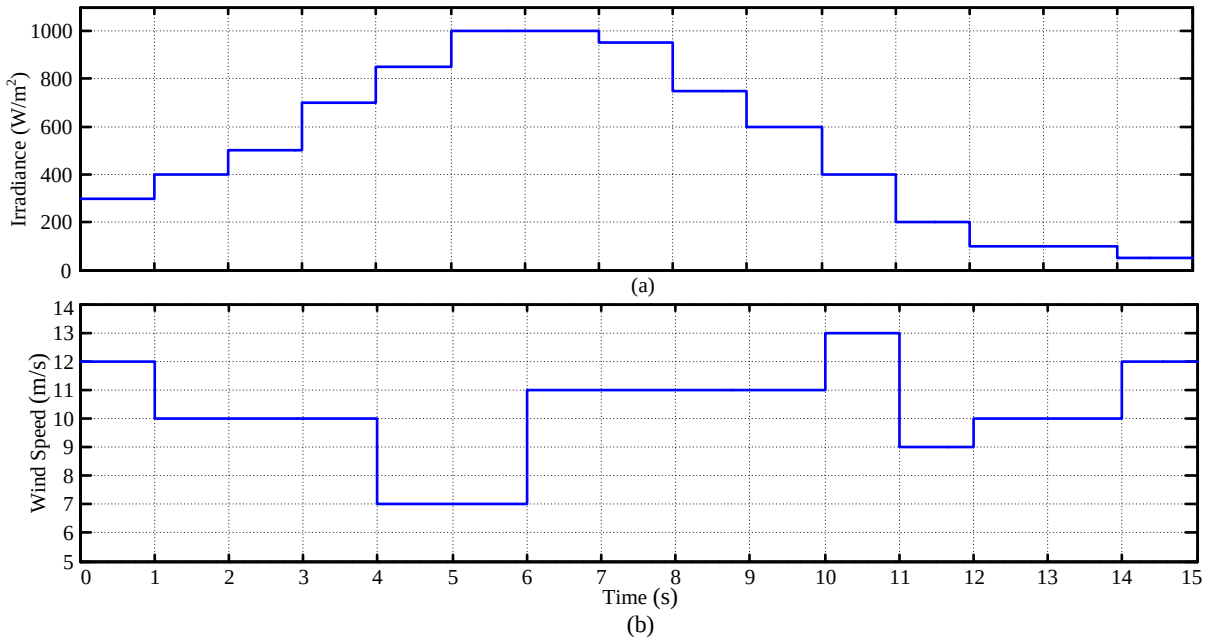

Fig. 15: changes in (a) solar irradiance, (b) wind speed

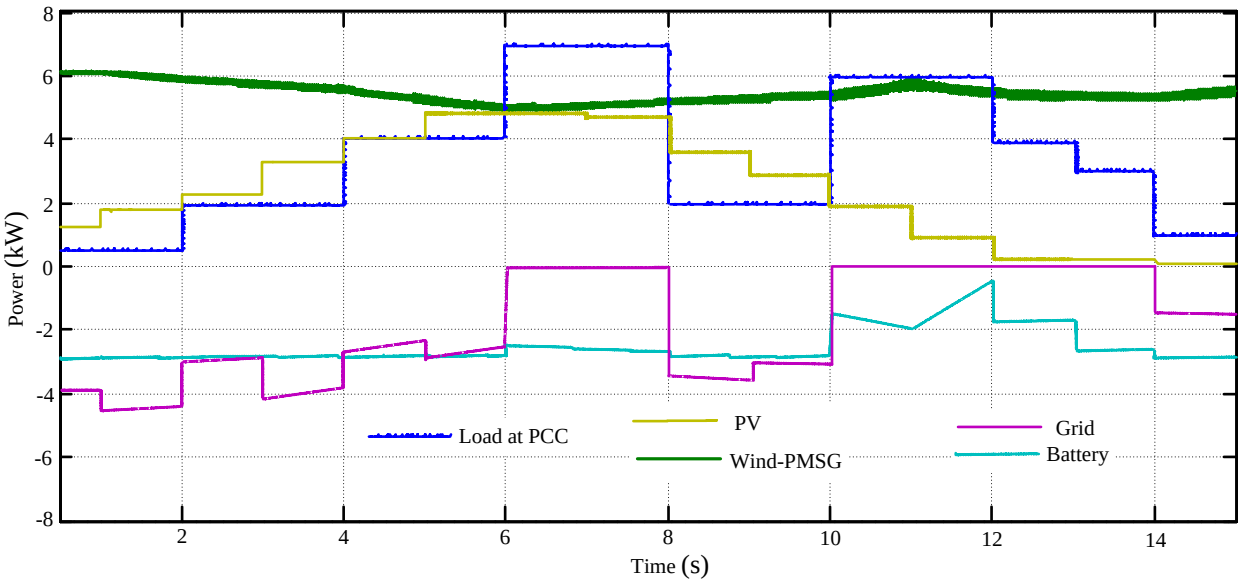

Fig. 16: Power diagram of load, PV, Wind-PMSG, Grid and battery

For better understand the results are taken under steady state, hence the starting time in Fig. 16 is not started from 0 sec. in this case, considered the initial SoC of battery as 0 percent and battery changing capacity is limited to 3 kW by setting the upper limit of limiter in Fig. 9. Hence, up to 3kW will be taken by battery from the surplus power by generation. The remaining power will be transmitted to grid. Moreover, the grid power is not allowed to charge the battery. Hence, grid only can take the power but cannot supply power to charge the battery. This condition is reflected between 6 sec to 8 sec and 10 sec to 14 sec in Fig. 16. If the surplus power is more than 3kW, then the rest of power will be transmitted to grid.

Case-3: Performance of inverter controller under unbalanced load connected at PCC:

The nature of load connected to PCC is always in unbalanced for 3 phases. This unbalanced load will consume unbalanced line currents from Grid lines, this will effect on grid voltages at PCC due to unbalanced line drops of Grid. From Fig. 12, the unbalanced current components are allowed through inverter. Hence the inverter currents will become unbalanced during load unbalanced at PCC. Therefore, this inverter controller can make grid currents balanced during unbalanced load connected to PCC. Making balanced currents at grid side will be helpful to maintain balanced voltages through balanced droop across transmission line. The unbalanced load connected to PCC is shown in Fig. 17 and corresponding balanced grid currents are depicted in Fig. 18. Moreover, the inverter can generate different modulation indexes to maintain balanced voltages at PCC. The respective instantaneous and RMS voltages at PCC are shown in Fig. 19 and Fig. 20 respectively. The connection of unbalanced load is applied to PCC at 1.0 sec in this case.

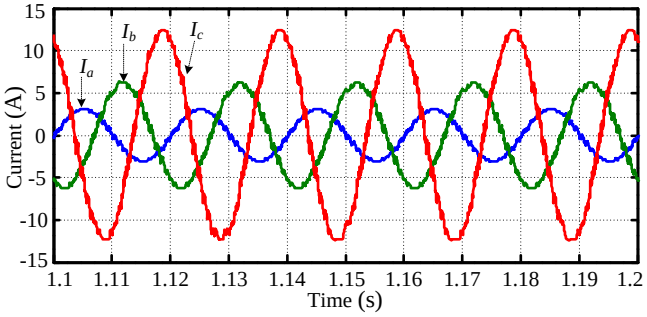

Fig. 17: Unbalanced load at PCC

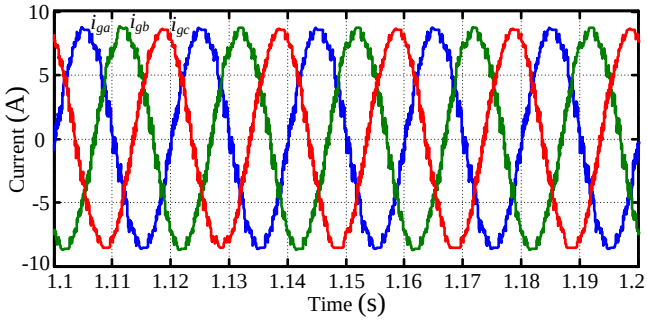

Fig. 18: instantaneous balanced Grid currents

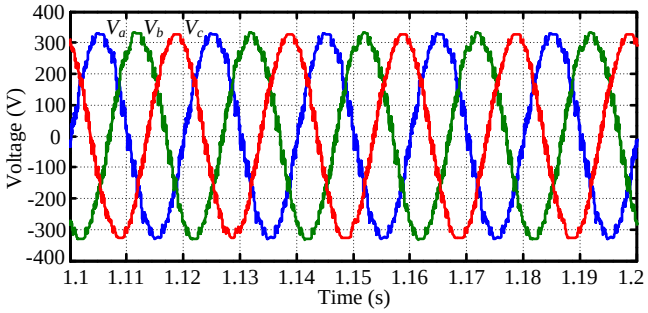

Fig. 19: instantaneous balanced voltages at Grid/PCC

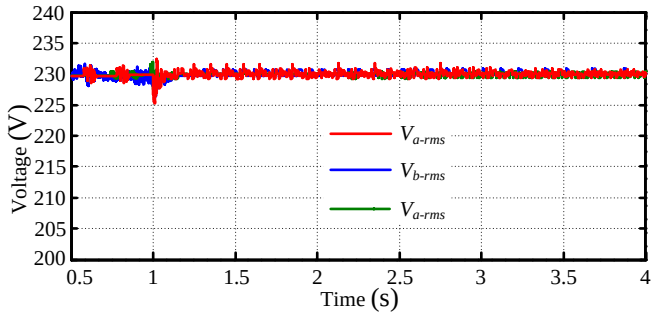

Fig. 20: RMS voltages at PCC/Grid

Case-4: Performance of inverter controller with reactive power load connected at PCC:

The inverter controller is tested under reactive power load connected at PCC. In order to compensate the reactive power from grid, the inverter needs to fulfill the load requirement or compensate the reactive power. The inverter controller is designed to compensate the reactive power at PCC by regulating RMS voltage at PCC. The reactive power component of current (i_q^*) is generated and compared with actual reactive component of current. With the help of these two components, inverter controller is generated direct axis component of voltage to generate required pulses. In order to compensate the reactive power, this voltage component is given to negative sign of summing point in Fig. 12. Hence, reactive power compensation can be achieved. For testing this case, the reactive power of 8kVAR is applied to PCC at t=2sec as shown in Fig. 21. From Fig. 21, it is observed that inverter is meeting the load reactive power which proves inverter is compensating load reactive power and reactive power supplied by grid becomes zero.

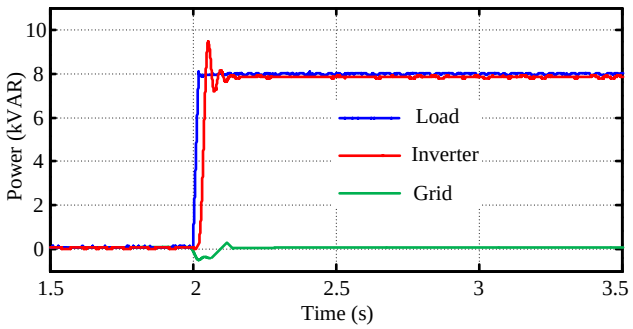

Fig. 21: Reactive powers of load at PCC, Inverter and Grid

Case-5: Performance of inverter controller with non-linear load connected at PCC:
In this case study, a non linear load with current profile of Fig. 22 (a) is connected to PCC. Due to this non linear load profile, the grid currents should not contain the harmonics. This can be achieved by inverter controller to operate as active power filter. The inverter 3-phase currents will be mitigates or compensates the non linear load by supplying the non linear profile of current trough inverter which is shown in Fig. 22 (b). Therefore, the grid currents will become sinusoidal as depicted in Fig. 22 (c).

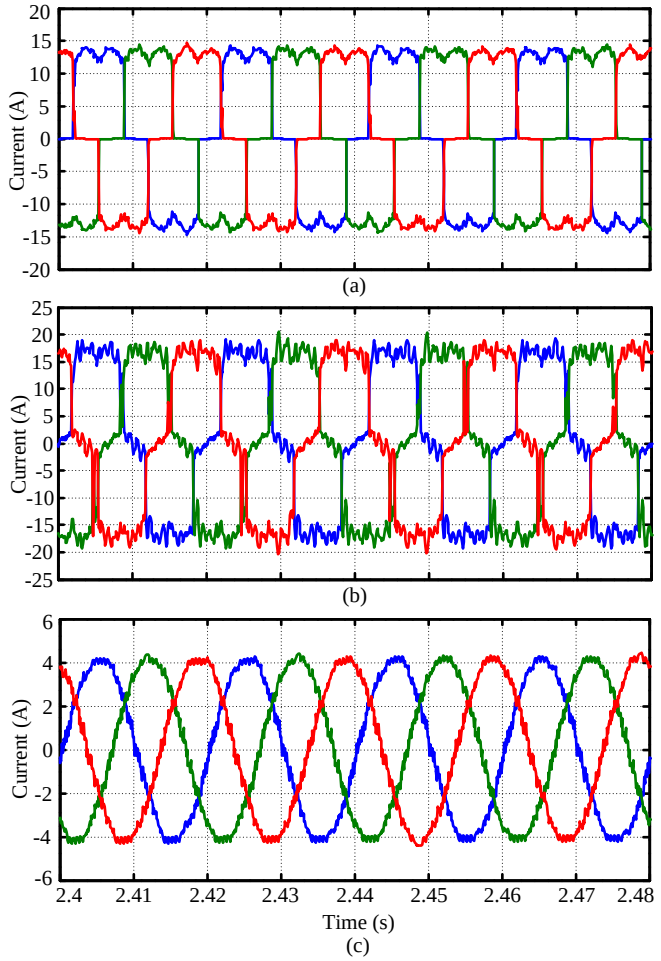

Fig. 22: (a) Non-linear load currents, (b) Currents flowing through inverter, (b) Grid currents

Case-6: System under stand-alone operation:
The system considered in this paper is grid connected, however, the chances are there to become the system isolated or stand-alone system when islanding occur. When the system is disconnected from grid, the system will become acts as stand-alone system and the battery will take care about the power management. In this case considered as islanding condition occurred at t=2sec and the unbalanced load connected at PCC. Moreover, the power consumed by load is more than the generation power from PV and Wind. In this situation, grid cannot supply the power since it is disconnected to PCC and the only option to manage the power by battery. Various powers are shown in Fig. 23 (a). After islanding condition i.e. t=2 sec, the battery is handling the power demand by load. Corresponding SoC of battery is presented in Fig. 23 (b). This can be possible by regulating dc-link voltage at its reference value as shown in Fig. 23 (c). as already mentioned as load as unbalanced, hence inverter controller needs to generate different modulation indexes to produce balanced RMS voltages at PCC as shown in Fig. 23 (d) and (e) respectively.

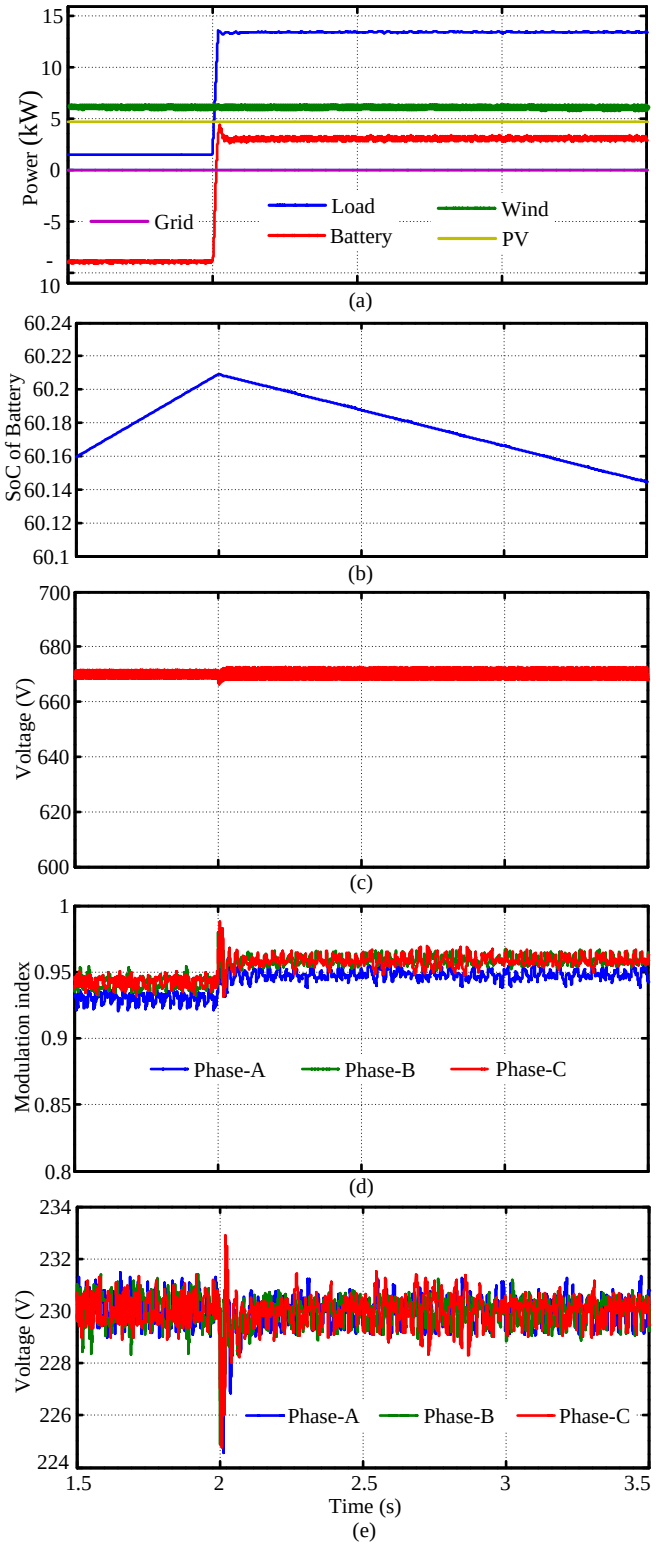

Fig. 23: System under stand alone mode: (a) Various powers, (b) SoC of battery, (c) Dc-link voltage, (d) Modulation indexes, (e) 3-phase RMS voltages

V. CONCLUSION

TS-Fuzzy based controllers are designed for grid connected wind-PV based hybrid system is presented in this paper. The inverter controller is designed for acting a DSTATCOM, active power filter as well as unbalanced load compensation. The detailed modeling of components are presented and discussed in this paper. The MPPT controller and algorithm of PV systems are integrated to DC-DC converter, hence no extra converter is required to extract the maximum power from PV system. The presented controllers are tested under different case studies.

References

[1] Müller S., Deicke M., and De Doncker Rik W. "Doubly fed induction generator system for wind turbines", *IEEE Industry Applications Magazine*, May/June, 2002, pp. 26-33.

[2] M. E. Haque, K. M. Muttaqi, and M. Negnevitsky, "Control of a standalone variable speed wind turbine with a permanent magnet synchronous generator," in *Proc. IEEE Power and Energy Society General Meeting*, Jul. 2008, pp. 20–24.

[3] M. E. Haque, M. Negnevitsky, and K. M. Muttaqi, "A novel control strategy for a variable-speed wind turbine with a permanent-magnet synchronous generator," *IEEE Trans. Ind. Appl.*, vol. 46, no. 1, pp. 331–339, Jan./Feb. 2010.

[4] C. N. Bhende, S. Mishra and S. G. Malla, "Permanent Magnet Synchronous Generator based Stand-Alone Wind Energy Supply System", *IEEE Transactions on Sustainable Energy*, Vol. 2, No. 4, pp. 361- 373, Oct. 2011.

[5] S. G. Malla and C. N. Bhende, "Voltage Control of Stand-Alone Wind and Solar Energy System", *Electrical Power and Energy Systems (Elsevier)*, Vol. 56, pp. 361–373, March 2014.

[6] S. G. Malla and C. N. Bhende, "Study of Stand-Alone Microgrid under Condition of Faults on Distribution Line", *International Journal of Emerging Electric Power Systems*, Issue 5, Vol. 15, 2014.

[7] S. G. Malla, et al., "Wind and Photovoltaic based Hybrid Stand-Alone Power Generation System", *IEEE: International Conference on Energy, Communication, Data Analytics and Soft Computing (ICECDS 2017)*,Chennai, India, 2017.

[8] S. G. Malla, C. N. Bhende and A. Kalam, "Mitigation of Power Quality Problems in Grid-Interactive Distributed Generation System", *International Journal of Emerging Electric Power Systems*, Vol. 17, Issue 2, pp. 165-172, 2016.

[9] S. G. Malla and C. N. Bhende, "Enhanced operation of stand-alone 'Photovoltaic-Diesel Generator-Battery' system", *Electric Power System Research (Elsevier)*, Vol. 107, pp. 250-257, Feb. 2014.

[10] P. A. Dahono and A. Purwadi, Qamaruzzaman, "An LC filter design method for single-phase PWM inverters," in *Proc. Int. Conf. Power Electronics and Drive Systems*, 1995, vol. 2, pp. 571–576.

[11] S. G. Malla et al., "SVM-DTC Permanent Magnet Synchronous Motor Driven Electric Vehicle with Bidirectional Converter", *Automation, Computing, Communication, Control and Compressed Sensing, IEEE Xplore, 2013*

[12] Bose B.K, Power Electronics and Motor Drives, Academic Press, Imprint of Elsevier, 2006.

[13] E. Muljadi, S. Drouilhet, R. Holz, and V. Gevorgian, "Analysis of permanent magnet generator for wind power battery charging," in *Proc. IEEE Industry Applications Society Annual Meeting*, 1996, pp. 541–548.

[14] A.M. Cross, P.D. Evans, and A. J. Forsyth, "DC link current in PWM inverters with unbalanced and non-linear loads," in *Proc. Inst. Elect. Eng. Electrical Power Applications*, Nov. 1999, vol. 146, no. 6, pp. 620–626.

[15] P. Enjeti and S. Kim, "A new DC-side active filter for inverter power supplies compensates for unbalanced and nonlinear loads," in *Proc. IEEE Industry Applications Society Annual Meeting*, 1991, vol. 1, pp.1023–1031.

[16] Dr. Siva Ganesh Malla, Priyanka Malla and Rajesh Koilada, "Solar Energy based Hybrid Electric Car: Part 1", *International Journal of New Technologies in Science and Engineering* (IJNTSE), Vol. 6, Issue 6, pp. 11- 25, Dec. 2019.

[17] Dr. Siva Ganesh Malla, Priyanka Malla and Rajesh Koilada, "Solar Energy based Hybrid Electric Car: Part 2", *International Journal of New Technologies in Science and Engineering* (IJNTSE), Vol. 6, Issue 6, pp. 26- 38, Dec. 2019.

[18] S. G. Malla, et al., "Solar-Hydrogen Energy based Hybrid Electric Vehicle",*IEEE: International Conference on Energy, Communication, Data Analytics and Soft Computing (ICECDS 2017)*,Chennai, India, 2017.

[19] N. Mohan, T. M. Undeland, and W. P. Robbins, *Power Electronics: Converters, Applications, and Design*. Hoboken, NJ: Wiley, 2002.

[20] S. G. Malla and C. N. Bhende, "A Stand-Alone Wind Energy System with Battery Storage", *International Conference on Power & Energy Systems and Applications*", 7-9 Nov. 2011, Pittsburgh, USA.

Author biography:

Dr. Siva Ganesh Malla was born on 1986 in Nagulapalli, Anakapalli, Visakhapatnam, Andhra Pradesh, India. He received the award of Ph. D from School of Electrical Sciences, Indian Institute of Technology (IIT) Bhubaneswar, Odissa, India in 2014. He got his B. Tech degree in Electrical Deportment from Jawaharlal Nehru Technological University Hyderabad in 2007 and M. Tech in Power Electronics and Electric Drives in Electrical Deportment from Jawaharlal Nehru Technological University Kakinada in 2010. Now he is working as a director of CPGC Pvt. Ltd, Visakhapatnam, Andhra Pradesh, India. His research interests are renewable energy sources, microgrid, power quality, electrical vehicles, biomedical signal processing, converters, power electronics, drives, optimization techniques and FACTS.

Google Scholar Page:
https://scholar.google.co.in/citations?user=iQ_gbcQAAAAJ&hl=en

Priyanka Malla was born on 1996 in Anakapalli, Visakhapatnam, Andhra Pradesh, India. She received her B. Tech in Electronics and Communication Engineering from Jawaharlal Nehru Technological University, Kakinada, India, in 2017. Presently she is working as Jr. GIS Engineer, Infotech, Cyient Ltd., Vizag, Andhra Pradesh, India. Her research interests are included in renewable energy sources, electrical vehicles, biomedical signal processing, optical communication and digital electronics.

Google Scholar Page:
https://scholar.google.co.in/citations?hl=en&user=dihA3DMAAAAJ